Mapping the fluid front and pressure buildup using 4D data on Norne Field

BÅRD OSDAL, ODDVAR HUSBY, HANS A. ARONSEN, NAN CHEN, and TRINE ALSOS, Statoil, Harstad, Norway

Norne Field, in the southern part of the Nordland II area in the Norwegian Sea approximately 100 km north of Aasgard Field, is producing from an FPSO. The main field is a horst block approximately 9 × 3 km (Figure 1). The reservoir rocks are sandstones of Lower and Middle Jurassic age. The hydrocarbon reserves consist of a gas cap (75 m), mainly situated in Garn Formation, and an oil leg (110 m), mainly situated in Ile and Tofte formations. The sandstones are very good quality with porosities and permeabilities of 25–32% and 200–2000 mD, respectively. Net-to-gross is close to 1 for most reservoir zones. Oil production started in 1997. The first 4D seismic survey was acquired in 2001, and 4D information has been actively used in subsequent reservoir management.

This paper will focus on the importance of tight integration of all disciplines for achieving good quality and repeatable 4D seismic data that can optimize new drilling targets and help obtain a more reliable reservoir simulation model.

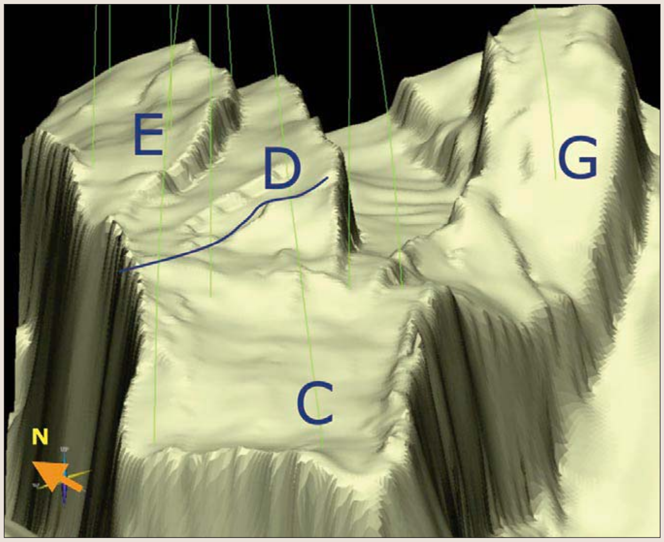

Figure 1. *Top reservoir map showing Norne horst block with four segments. G segment contains only oil in the uppermost Garn reservoir. Segment C, D, and E have 75 m of gas and 110 m of oil.*

Acquisition. The initial seismic survey was conducted in 1992 using a dual source and three streamers separated by 100 m. This was a big 3D exploration survey and was not, at that time, thought of as a 4D baseline survey. Three monitor surveys have been collected since the field began producing—in 2001, 2003, and 2004. All surveys were acquired with the WesternGeco Q-marine system. A single source and six steerable streamers separated by 50 m were used on all monitor surveys. This configuration repeated the base survey as much as possible. However, it was decided not to steer to repeat the feathering of the base survey. Instead all lines were acquired as close as possible to zero feather, because this is much easier to repeat. The first Q-acquisition in 2001 was considered the base Q-survey, and all new surveys repeat this geometry as accurately as possible.

Undershooting of the Norne production platform was performed in 2001, 2003, and 2004. Figure 2a shows the feathering difference between the base survey and the Q acquisition in 2003 (left), and between the Q acquisitions in 2001 and 2003 (right). Much larger feathering differences are seen with the base survey than between the Q-marine surveys. As seen in Figure 3, this clearly influences the amount of nonrepeatable noise in the 4D data. The repeatability between the Q-marine surveys is clearly better than between the base and Q-surveys. Average nrms for base versus Q is approximately 40%; the corresponding number for Q versus Q is 19–21%.

Detailed monitoring of source and feathering repetition is performed during acquisition. A raw difference stack of the line is produced shortly after the line is acquired. In 2004 this 4D difference was compared to the 2001–2003 difference and was very useful in deciding if a newly acquired line should be rejected or not. The lesson learned was clearly that, in 4D, some swell noise can be accepted, because this can effectively be removed in processing. Geometry failure (source and/or feathering mismatch), however, is more difficult to tolerate.

All three undershoots of the Norne FPSO used a two-boat operation (one conventional shooting boat and one Q-marine streamer boat). Again the acquisition geometry was repeated as accurately as possible, but good repetition in this area was much more difficult to achieve than in the main area covered by a one-boat operation. Figure 2b shows inline deviation (dis-

for the main area and the undershoot area. Figure 2c shows the crossline deviation (distance in crossline direction) between far offsets (middle cable) of 2003 and 2004 for the main area and the undershoot area. More deviation between the surveys can be seen for the undershoot area than for the main area. This can be explained by the much more difficult timing challenges involved with two-boat operations than with one boat. On the final processed 4D line, repeatability is a little worse in the undershoot area between 2003 and 2004 than between 2001 and 2003. The same undershoot vessel (and same source) was used in 2001 and 2003, but a new undershoot boat (with a different source) was used in 2004. This caused a lot more work in the signature-matching process than we expected.

The undershoot vessels were not Q-boats and did not have the calibrated marine source (CMS). A single modeled far-field signature is therefore used for the signature deconvolution in the undershoot area. The amplitude and timing relationship between the modeled far-field signature and the CMS signature is not straightforward and is very difficult to estimate properly. The lesson learned here is that either the same conventional source should be used each time, or that the same CMS source used in the main area be used in the undershoot area.

In the main area, slightly better repeatability can be seen for 2003–2004 than for 2001–2003 (Figure 3). For the main field area (yellow polygon), mean nrms of 19% was measured for 2003–2004; the corresponding number for 2001–2003 was 21%. This is due to better accuracy of source and receiver position repeatability. Figure 4 shows the radial (distance between points) source and far-offset cumulative differences between the surveys. In 2004 more than 70% of the shots were within 5 m of the shots in 2003. The corresponding number was 50% for 2003 and 2001. For the far-offset repetition, approximately 70% of the shots in 2004 were closer than 25 m to the 2003 shots. This figure was approximately 60% for 2003 compared

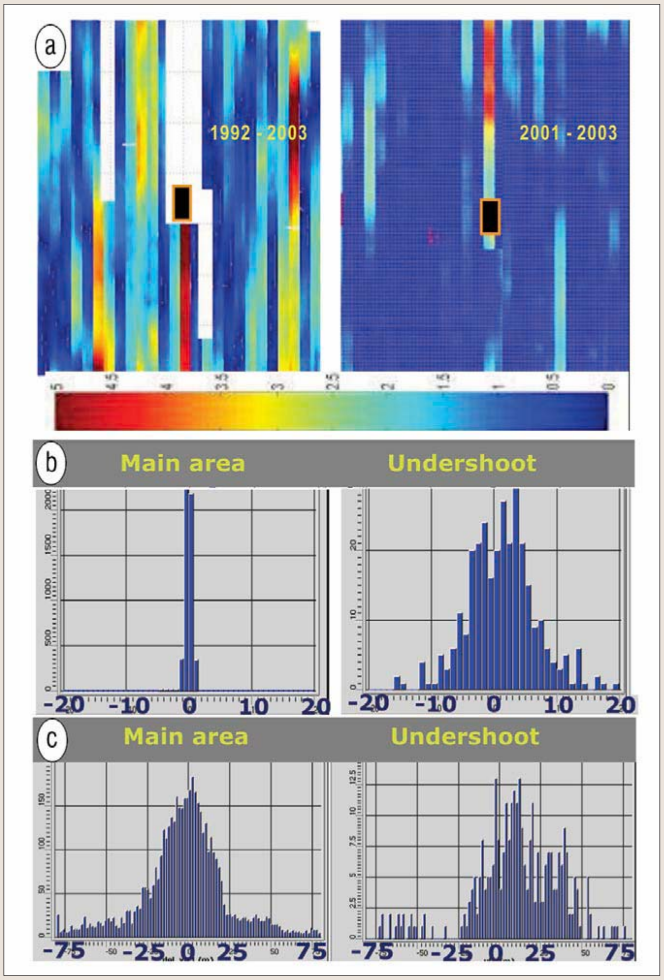

Figure 2. (a) Left is feathering difference between base and 2003, and right is difference between 2001 and 2003. (b) Inline source deviation of 2003 and 2004 of main area (left) and undershoot area (right). (c) Far-offset crossline deviation of 2003 and 2004 of main area (left) and undershoot area (right).

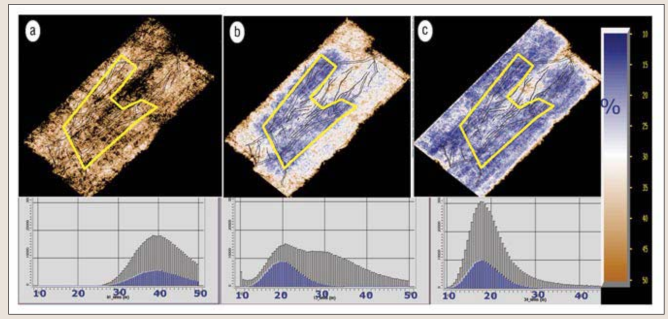

Figure 3. The nrms maps and nrms histograms measured on the 4D data in overburden of (a) base and 2001, (b) 2001 and 2003, and (c) 2003 and 2004. Blue data points in the histogram are related to the yellow polygon on the map.

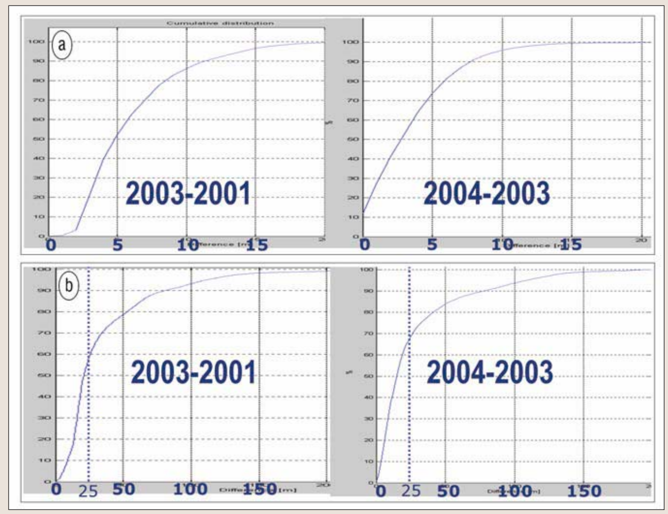

Figure 4. Cumulative radial (a) source difference and (b) far-offset difference between vintages.

Processing. The best way to interpret the OWC at Norne is by using the difference data, and this requires careful 4D processing to enhance the production-related 4D differences. All Norne vintages go through the same processing sequence at WesternGeco.

During processing, it is essential to test processing algorithms on all vintages so that 4D difference displays can be analyzed and compared.

In general, adaptive processes should be avoided and deterministic processes preferred. Figure 5 shows the effect of tau-p decon on the 4D data. The process is applied on all vintages and analyzed on the 4D differences. The decon clearly helps remove multiples, but it also degrades the 4D effect of the rising OWC (blue circle). The Norne data are heavily contaminated by diffracted multiples, requiring multiple attenuation and several passes of Radon. The best solution at Norne was to apply 2D SRME (Figure 5c). Even though this is an adaptive process, testing showed that it preserved the 4D signal well and was most effective in removing the multiples. It should be noted that the repeated acquisition geometry of zero feather is clearly an advantage for optimum results from SRME in a 4D sense.

4D binning is important in 4D processing. To obtain good repeatable 4D data, it is very important to select the pair of traces between two vintages that best match in terms of source

ing an overfold area compared to the situation in which non-repeating traces are thrown away. Pairs of traces between the two vintages that do not match in acquisition geometry will clearly degrade the 4D difference.

4D interpretation strategy. The rise of the OWC at Norne can most effectively be interpreted using the 4D difference data. Figure 7a shows seismic modeling (stacks) of varying rise of the OWC (0–70 m). The new OWC is almost impossible to locate on these stacks. However, if the 4D differences are used, the geology can be cancelled and the new and original OWC are left in the data as shown in Figure 7b. Figure 7c shows a 2003 line through a water injector. The 2003 OWC cannot be interpreted on this line. On the 2001–2003 difference (Figure 7d), however, the 2003 OWC is interpretable. Figure 7e shows some synthetic modeled difference data in the injector based on repeated saturation logging in 2000 and 2002. The left curves in Figure 7e show the relative change in acoustic impedance between base and 2000 (blue) and base and 2002 (black) surveys. A complete flushing of the oil with water causes an acoustic impedance change of 7–8%. Figures 7c–e are plotted at the same depth scale. Even though the timing of the repeated saturation logging does not coincide with the timing of the 4D data, this 4D modeling very much confirms that our OWC interpretation strategy is valid.

A reservoir simulation 4D modeling approach is used on Norne to optimize the 4D interpretation and reservoir simulation history matching. Seismic modeling of the simulation

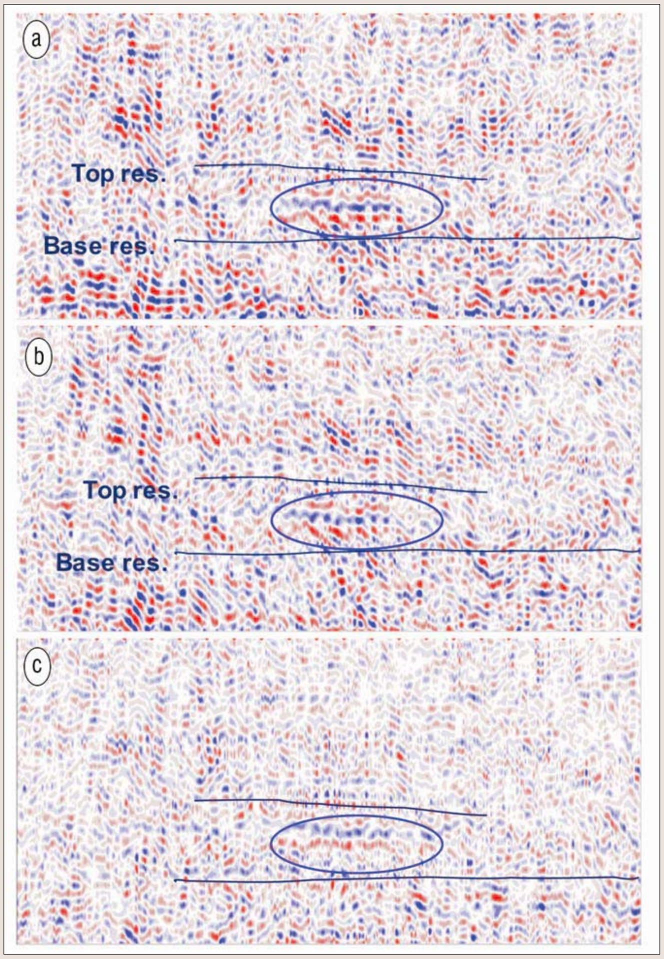

Figure 5. *(a) Radon stack. (b) Radon and tau-p decon. (c) Radon and 2D SRME. Blue circle highlights the 4D effect of a rise of the OWC.*

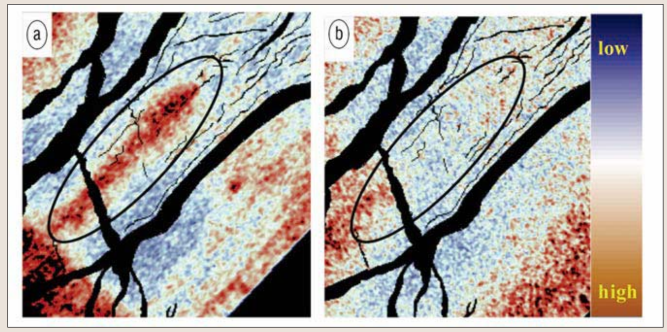

Figure 6. *The nrms map showing an overfold area with (a) all data used in the processing and (b) 4D binning applied and nonrepeating traces thrown away.*

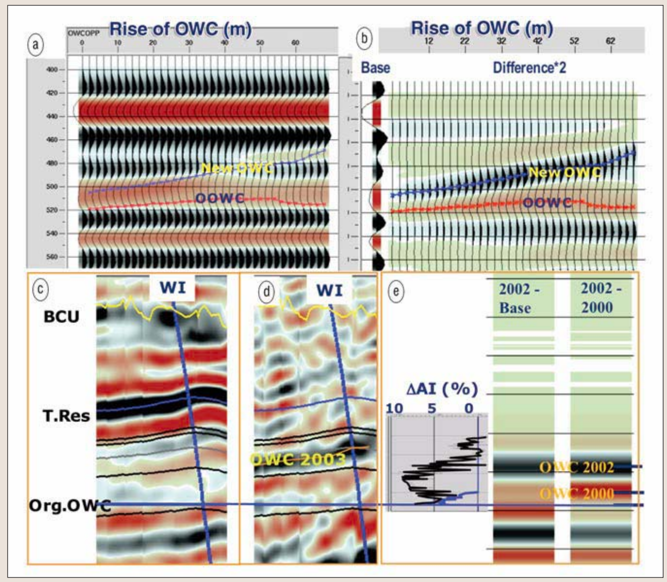

Figure 7. *(a) Seismic modeling for varying rise of OWC from 0–70 m. (b) Seismic differences for varying rise of OWC and the first base trace. (c) 2003 4D data around an injector. (d) 2001–2003 4D difference around same injector. The 2003 OWC can clearly be interpreted here. (e) Left curves show change in acoustic impedance in % from base to 2000 (blue curve) and base to 2002 (black curve). Seismic modeling on the right show differences between base and 2002 and 2000–2002.*

simulation model does not coincide with the 4D data and production data. Both seismic reflection amplitudes and acoustic impedance are compared. A Norne rock model and the Gassmann equation are used for calculating seismic parameters. The SimPli method from Norsar (Drottning et al., 2004) is used to model seismic at different vintages. Seismic modeling is important for history matching and is also a guide to how the 4D difference data can be interpreted and understood.

Seismic modeling in pilot wells and in wells with repeated saturation logging (as in Figure 7e) is also very important as an interpretation guide and to validate the 4D interpretation.

Case studies. The first study is from the E segment (Figure 1). Based on 4D data from 2003, it was decided to drill infill production well E-3CH. The well location was confirmed to be good on the 2004 data, and the well was drilled with success during the spring of 2005. When the 2003 4D data were analyzed, a clear difference was seen between the 4D data and the reservoir simulation model. Figure 8 shows this comparison for a line through well E-3CH from the simulation model and the 4D data. A map showing the position of this well is shown in Figure 8f. Figure 8a shows water saturation from the simulation model in mid-2003. Figure 8b shows modeled seismic 4D difference of the simulation model. Figure 8c shows the real 4D difference data (2001–2003), and here the OWC from 4D (blue line) clearly can be interpreted deeper than in the simulation model (yellow line). In the simulation model at that time, fault A (Figure 8f) was open and the water flowed easily from the water injector F-1H through fault A.

water from F-1H therefore flowed along fault A instead of through it (red arrow in Figure 8f). This is confirmed by tracer data in the area. By decreasing the fault transmissibility of fault A and extending it farther to the main fault (B), a new simulation model was created that had a much better match with the 4D data (Figures 8d and 8e). The green line is OWC on the new simulation model, and this matches the 4D OWC (blue line). The location of E-3CH was now also good in the simulation model.

The new simulation model also improved the water cut and pressure match in the area. This is shown for two wells in Figure 9. Prior to drilling the production well, it was decided to drill a pilot well to check the OWC. The pilot well confirmed the OWC level as interpreted from the 4D data and predicted from the new simulation model.

Figure 10 summarizes the results from E-3CH after six months of production. The figure compares the actual oil production and water cut with the prediction from the old and new simulation models. The new simulation model predicts the real observation clearly better than the old model. History matching using the 4D data in this area was also described in an earlier paper (Lygren et al., 2005).

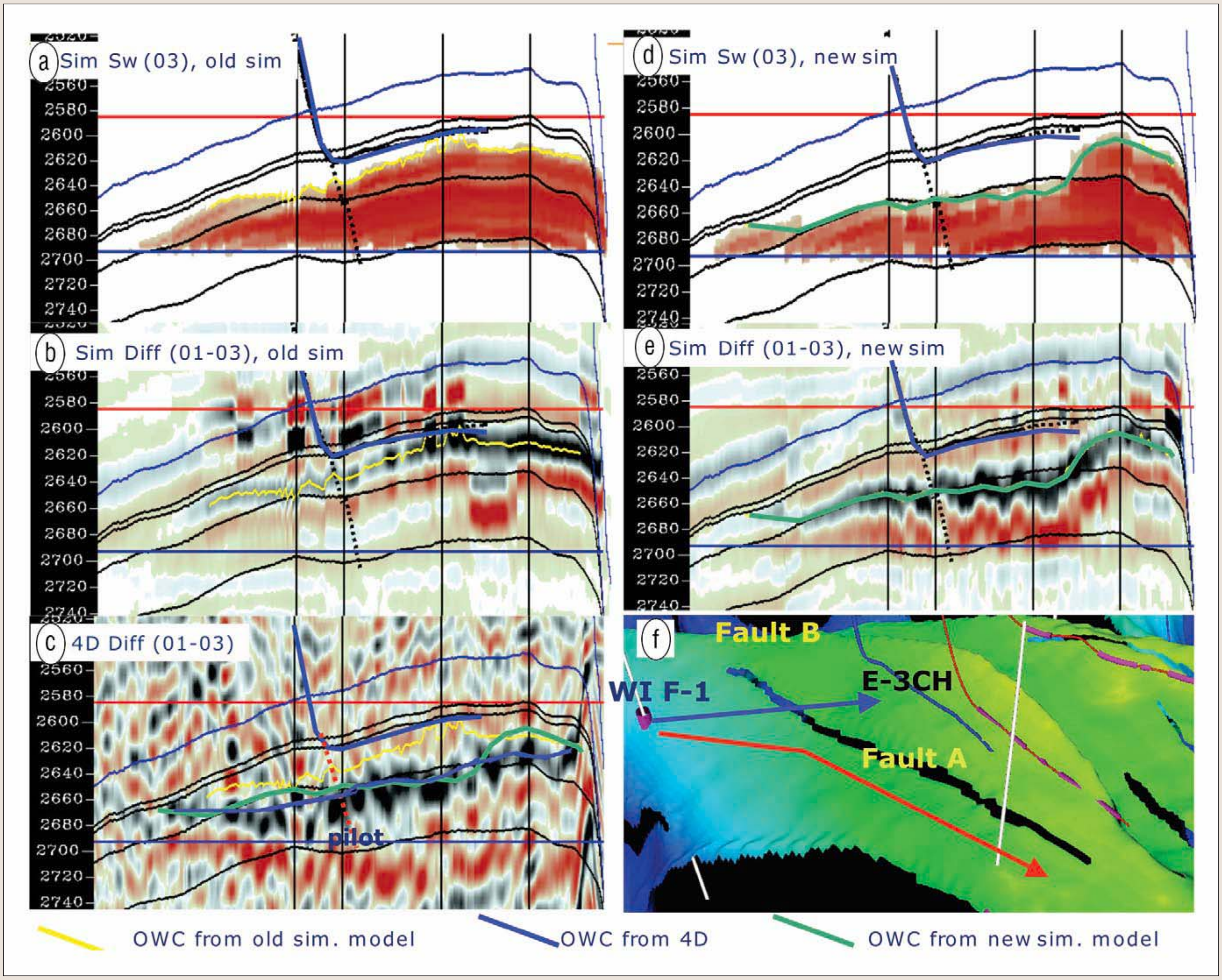

Figure 8. (a) Water saturation (red is high saturation) of old simulation model and (b) seismic modeling (4D difference) of old simulation model. (c) Real 4D difference data. (d) Water saturation (red is high saturation) of new simulation model and (e) seismic modeling (4D difference) of new simulation model. (f) Top reservoir map.

ment (Figure 1). A horizontal producer was drilled in the autumn of 2003. The first planned location was based on the 2001 4D data and the simulation model available at that time. Figure 11a shows the water saturation from the old simulation model in 2003. A carbonate cemented barrier is between Ile and Tofte formations. Pressure changes over the barrier were observed in several wells in the area, and it was expected to be a barrier for the water beneath. The first well location was therefore placed in the highly porous and permeable Lower Ile Formation, above the carbonate cemented zone. Figure 11b shows the 2001–2003 fast track onboard-processed 4D acoustic impedance difference data received seven days after the last shot of the 2003 acquisition. Red indicates increase in impedance from 2001 to 2003 and is related to water replacing oil. It is clear that the water indeed passed through the carbonate cemented zone and flooded the lower part of Ile Formation. It is also evident that the toe of the originally planned well path seems to be in the water zone. To avoid early water production, the well location was moved upward and away from the water front (yellow line). This new well location was identified 14 days after the acquisition. The well was drilled successfully in the oil zone, and the first year after start up it produced with a rate of approximately 4000 Sm^3/d

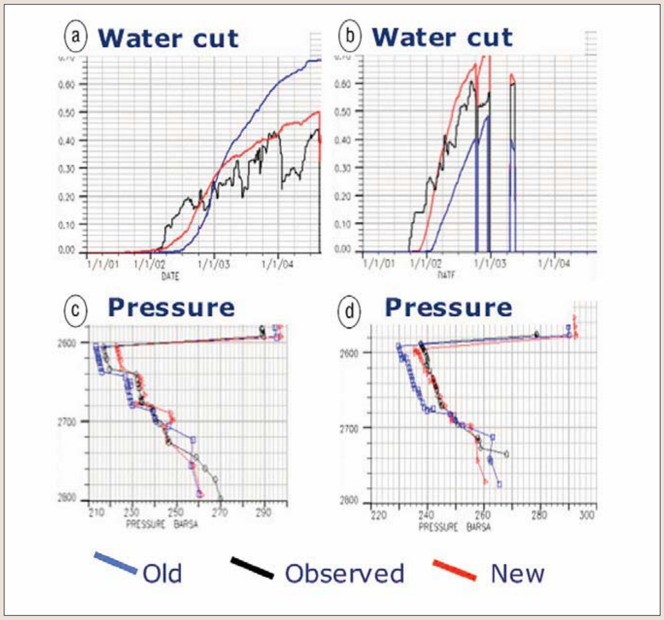

Figure 9. (a) and (b) water cut match and (c) and (d) pressure match for

breaking through the barrier can be that the area contains more small-scale faulting than can be observed in the seismic data. The carbonate cemented zone is thin (approximately 20 cm) and tight, and even small-scale faulting can break this barrier and allow the water to flow through. By introducing more small-scale faulting into the simulation model, the observation from the 4D data can be better matched (Figure 11c).

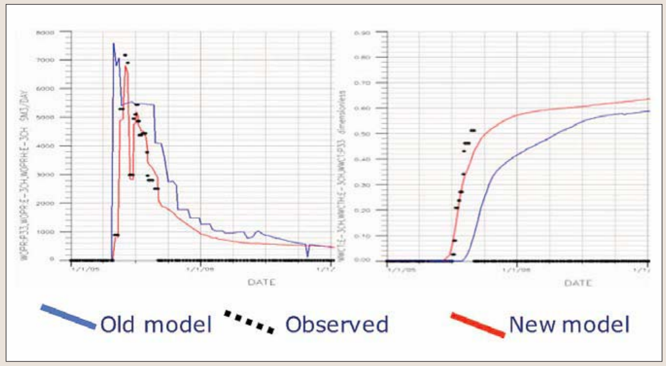

Figure 10. *Left plot shows oil production, and right plot shows water cut for the well E-3CH. The new simulation model has predicted observations more accurately.*

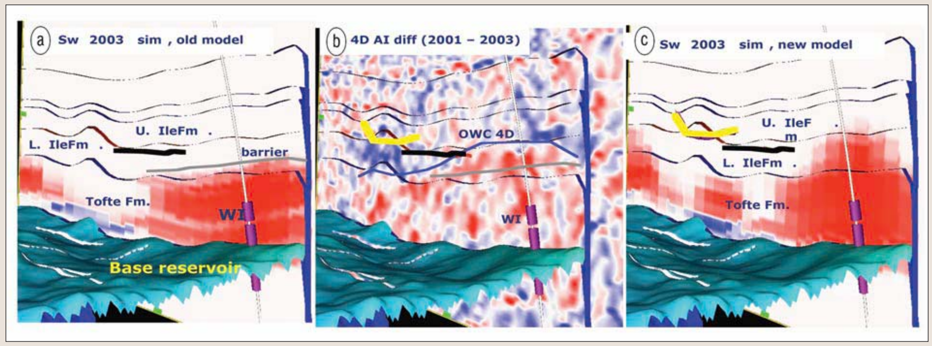

Figure 11. *(a) Water saturation of old simulation model. Red is high water saturation. (b) 4D acoustic impedance difference. Red is increase in impedance from 2001 to 2003, indicating water replacing oil. (c) Water saturation of new simulation model. Red is high water saturation.*

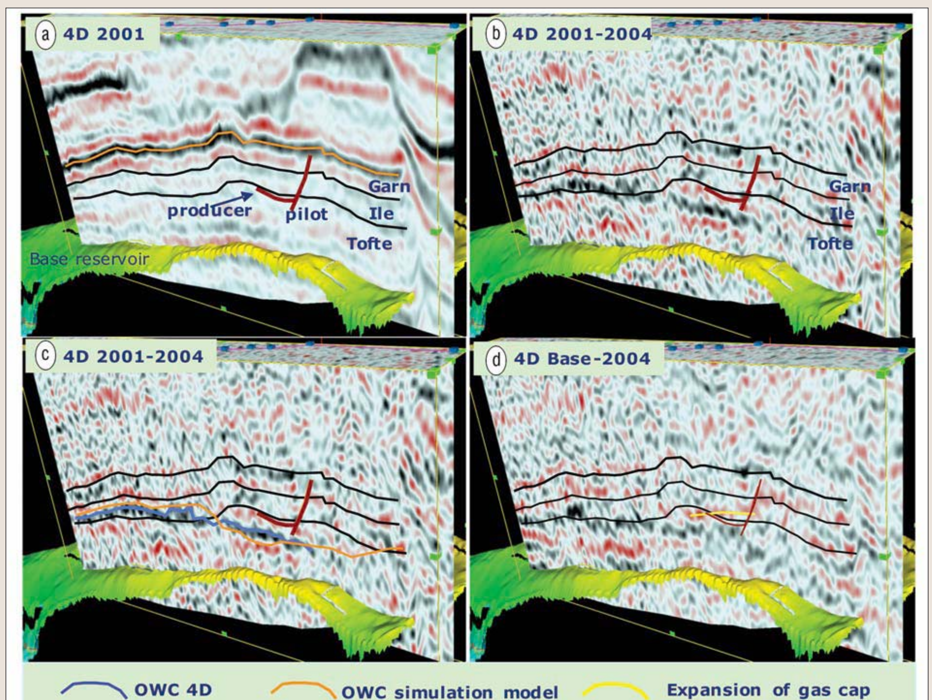

Figure 12. *(a) 4D data 2001. (b) 4D difference 2001–2004. (c) 4D difference 2001–2004 with OWC interpretation. (d) 4D difference between base and 2004 with interpretation of gas cap expansion (yellow).*

The third case study is from the northwestern part of C segment (Figure 1). The 4D data in 2003 and 2004 indicate that the upper part of Tofte Formation was undrained, and a new producer was therefore scheduled to be drilled in this area in the autumn of 2005. Figure 12 shows 4D amplitude and 4D difference data from a line through the well. The OWC is interpreted to be in the lower part of Tofte Formation. As pointed out earlier, the OWC is very difficult to interpret on each vintage (Figure 12a). The OWC is much clearer and interpretable on the Q versus Q differences in Figures 12b–c. Much gas was injected in this area prior to the 2001 acquisition. This gas is also seen in the area in 2004. The base-2004 difference (Figure 12d) shows this expansion of the gas cap (yellow line). Prior to drilling the horizontal producer, a pilot well was drilled into Tofte Formation to check the OWC and to take pressure measurements. Due to high pressure in the lower part of the formation, the pilot well had to be stopped before the OWC was reached. However, this pilot well confirmed that the upper part of Tofte Formation is undrained, as predicted by the 4D data. The pilot well also showed some gas cap expansion. Much of the water flooded into this area is most likely coming from the north. The new simulation model has fairly good agreement with the 4D data as indicated in Figure 12c by comparing the OWC from the 4D data and the simulation model (blue and red lines). The horizontal producer began production in January 2006. By the end of February 2006, the well was producing approximately 5500 Sm^3/d with no water.

The last case study is from G segment (Figure 1) in what was initially an undersaturated reservoir in Garn Formation (thickness of 25–30 m). No initial gas cap is present. Well E-4 (Figure 13) began production in July 2000. When the first 4D repeat survey was shot in 2001, the pressure had depleted below the bubble point to approximately 200 bar. Figure 13a shows the change in impedance between the base and 2001 surveys. Blue is related to impedance decrease. This can be explained by gas out of solution due to the pressure drop. This anomaly outlines the whole segment, and it shows that there is no pressure barrier between the E-4 producer and the rest of the oil in the segment. Figure 13b shows the amount of gas in the the 2001 4D data.

Well F-4 began water injection in the autumn of 2001, and this resulted in a general pressure increase in the G segment. A PLT in F-4 in 2005 reported a pore pressure of 300 bar. Figure

DOCKET ALARM

Explore Litigation Insights

Docket Alarm provides insights to develop a more informed litigation strategy and the peace of mind of knowing you're on top of things.

Real-Time Litigation Alerts

Keep your litigation team up-to-date with **real-time alerts** and advanced team management tools built for the enterprise, all while greatly reducing PACER spend.

Our comprehensive service means we can handle Federal, State, and Administrative courts across the country.

Advanced Docket Research

With over 230 million records, Docket Alarm's cloud-native docket research platform finds what other services can't. Coverage includes Federal, State, plus PTAB, TTAB, ITC and NLRB decisions, all in one place.

Identify arguments that have been successful in the past with full text, pinpoint searching. Link to case law cited within any court document via Fastcase.

Analytics At Your Fingertips

Learn what happened the last time a particular judge, opposing counsel or company faced cases similar to yours.

Advanced out-of-the-box PTAB and TTAB analytics are always at your fingertips.

API

Docket Alarm offers a powerful API (application programming interface) to developers that want to integrate case filings into their apps.

LAW FIRMS

Build custom dashboards for your attorneys and clients with live data direct from the court.

Automate many repetitive legal tasks like conflict checks, document management, and marketing.

FINANCIAL INSTITUTIONS

Litigation and bankruptcy checks for companies and debtors.

E-DISCOVERY AND LEGAL VENDORS

Sync your system to PACER to automate legal marketing.

WHAT WILL YOU BUILD? | **sales@docketalarm.com** | **1-866-77-FASTCASE**

fastcase®
Smarter legal research.